Supramolecular Chemistry
Publication details, including instructions for authors and subscription information:
http://www.informaworld.com/smpp/title~content=t713649759

Potassium Extraction by a Cryptand to Supercritical CO_2. The Role of Counterions Investigated by MD Simulations at the Water/SC-CO_2 Interface

N. Galand[a]; G. Wipff[a]
[a] Institut de Chimie, Strasbourg, France

To cite this Article Galand, N. and Wipff, G.(2005) 'Potassium Extraction by a Cryptand to Supercritical CO_2. The Role of Counterions Investigated by MD Simulations at the Water/SC-CO_2 Interface', Supramolecular Chemistry, 17: 6, 453 — 464
To link to this Article: DOI: 10.1080/10610270500163993
URL: http://dx.doi.org/10.1080/10610270500163993

Supramolecular Chemistry, September 2005 Vol. 17 (6), pp. 453–464

Potassium Extraction by a Cryptand to Supercritical CO_2. The Role of Counterions Investigated by MD Simulations at the Water/SC–CO_2 Interface[a]

N. GALAND and G. WIPFF*

Institut de Chimie, 4 Rue B. Pascal, 67 000 Strasbourg, France

Received (in Austin, USA) 19 January 2005; revised form 6 May 2005; Accepted 6 May 2005

We present a molecular dynamics study of the K^+ extraction by the 222 cryptand, comparing different counterions X^- at the supercritical-CO_2/water interface: X^- = picrate "Pic^-" *vs* perfluorooctanoate "PFO^-" *vs* chlorinated cobalt dicarbollides CCD^- *vs* Cl^-. The distribution of the free K^+X^- salts is also investigated, showing different distributions, depending on the hydrophobicity of X^-. The Pic^- and CCD^- anions markedly concentrate at the interface, as do the amphiphilic PFO^- anions, thus attracting K^+ cations near the interface. Similarly, in the M^+ CCD^- series with M^+ alkali cations, the less hydrophilic Cs^+ cations sit closer to the interface than do Na^+ or K^+. The simulations confirm the strong affinity of the 222 cryptand and of the $K^+ \subset 222$ cryptates for the interface, with marked counterion effects. The most remarkable result is the partitioning of the cryptates and CCD^- anions to the CO_2 phase, i.e. on the pathway to full extraction. With the other studied anions, no "extraction" proceeds. When compared to the K^+ or Sr^{2+} extraction by 18-crown-6, the results show that the effectiveness of X^- depends on its relationship with the complex: CCD^- forms separated ion pairs with $K^+ \subset 222$, whereas PFO^- forms intimate ion pairs with $K^+ \subset 18C6$ and $Sr^{2+} \subset 18C6$. Addition of hydrophobic salts like CCD^- Cs^+ and cryptands in excess enhances the K^+ extraction. Finally, the simulations on $K^+ \subset 222$, CCD^- solutions at increasing CO_2/water ratio shows the evolution from a "flat" interface to microemulsions, leading to the extraction of cryptates.

INTRODUCTION

Most studies on molecular recognition, a founding theme of supramolecular chemistry concerned the elucidation of the circumstances under which cations can be transported from an aqueous to an organic phase or to lipophilic membranes [1–8]. This led to the development of synthetic molecules which act as selective hosts towards cationic guests, based on the lock-and-key complementarity principle [9–12]. The formation of a complex is not sufficient, however, as the latter must be hydrophobic enough to partition to the organic phase, and the electro-neutrality of the source and receiving phases must be conserved. Thus, cation extraction by non-ionizable neutral hosts proceeds with suitable counterions X^- whose nature may not only determine the efficiency of the extraction process, but also the cation extraction selectivity. Discussions can be found in refs [13–15]. While classical extraction generally proceeds towards organic solvents which are not miscible with water (e.g. halogenated alkanes, aliphatic or aromatic solvents), new routes have been recently reported in the context of "green chemistry" with supercritical-CO_2 "SC–CO_2", an easily recoverable, available and cheap solvent which appears as a promising alternative to conventional solvents [16–19]. Generally the ligands used for classical extraction of cations also extract the latter to SC–CO_2, as shown for 18-crown-6 ("18C6") derivatives, diketonate or phosphoryl containing ligands [20]. Extraction can also be conducted to room temperature ionic liquids, presumably via another mechanism, involving cation exchange with the solvent, thus with no effect of X^- counterions [21,22].

*Corresponding author. E-mail: wipff@chimie.u-strasbg.fr

[a]This paper is dedicated to the memory of B. Dietrich. He contributed from the beginning with J.-P. Sauvage to the development of cryptate and supramolecular chemistry in the group of Prof. J.-M. Lehn in which one author (WG) started "*ab Initio*" calculations in 1969.

ISSN 1061-0278 print/ISSN 1029-0478 online © 2005 Taylor & Francis
DOI: 10.1080/10610270500163993

The present paper focuses on a prototypical system, the K^+ extraction by the *222* cryptand, whose complexation and extraction properties have been extensively studied and can be considered as the cornerstone of supramolecular chemistry [2,3,5,23,24]. Based on computer modeling simulations, we want to investigate the role of X^- counterions on the assisted cation extraction, focusing on the water-"oil" interface, where "oil" is modeled by $SC-CO_2$. As there is so far, to our knowledge, no experimental reports with cryptands to $SC-CO_2$, the studied systems are hypothetical, but display marked analogies with classical extraction systems. We recently investigated the effect of anions on the K^+ *vs* Sr^{2+} extraction by 18C6 to $SC-CO_2$ and found very important effects [25]. Efficient Sr^{2+} extraction was observed with perfluorooctanoate PFO^- anions (Fig. 1), which form intimate ion pairs with $Sr^{2+} \subset$ 18C6 complexes in the CO_2 phase [26,27]. In the $K^+ \subset$ *222* cryptates the cation is more shielded than in $M^{n+} \subset$ 18C6 complexes, and we want to investigate whether the CO_2-philic PFO^- anions can also promote the extraction of $K^+ \subset$ *222* cryptates with which ion pairing seems more difficult. The anions considered here are Cl^-, picrate Pic^-, chlorinated cobalt dicarbollide CCD^- and PFO^- (see Fig. 1). The three first ones have been tested for classical extraction studies on related systems, PFO^- has been used for extraction to $SC-CO_2$ [26,27]. While Cl^- is presumably too hydrophilic for efficient extraction, Pic^- or phenolate analogues has been extensively used for classical extraction [28] but not, to our knowledge, for supercritical fluid extraction. Less common is the "peanut shaped" CCD^- anion developed in the context of nuclear waste partitioning and used as such or via derivatives bearing complexation sites [29–32]. We first consider the M^+X^- and M^+ CCD^- electrolytes at the CO_2-water interface, in order to compare their distribution as a function of X^- for a given cation (K^+), and as function of the cation ($M^+ = Na^+$ to Cs^+) for a given anion (CCD^-). This is important in the context of assisted cation extraction as the cation concentration near the interface must be sufficient to form a complex with the extractant. This is also of interest for interfacial electrochemistry, due to the potential created by the M^+ and X^- ions at the interface. We then consider the $K^+ \subset$ *222* complexes near the interface, in order to investigate whether their migration to the oil phase can be promoted by some of the studied X^- anions. More complex mixtures of the $K^+ \subset$ *222* solutions involving an excess of *222* cryptands or a background electrolyte will be also investigated. Finally, we investigate the evolution of the $K^+ \subset$ *222*, CCD^- solutions at high CO_2/water ratio, in order to analyze the evolution of the interface and the distribution of the solutes, with their possible extraction to the CO_2 phase.

METHODS

The simulations were performed with the modified AMBER7.0 software [33] where the potential energy U is described by a sum of bond, angle and dihedral deformation energies, and pair wise additive 1-6-12

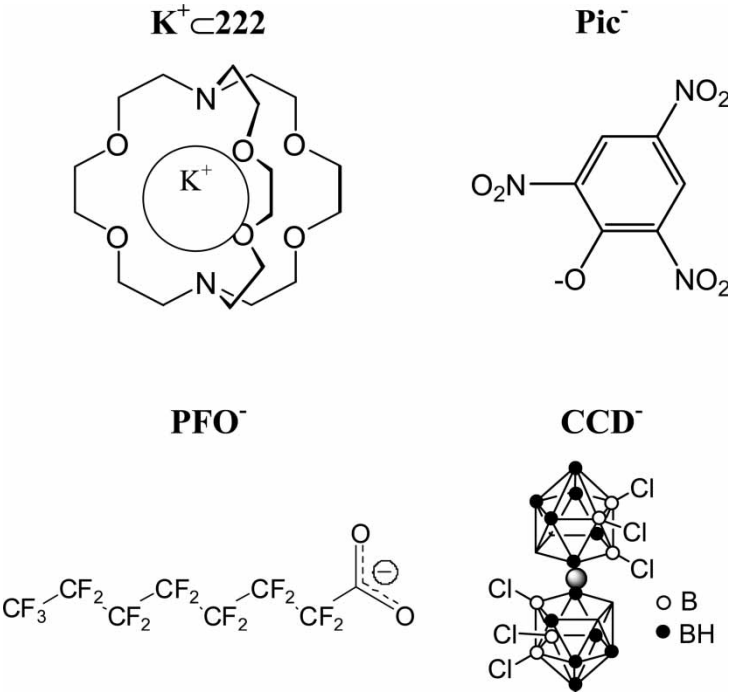

FIGURE 1 Studied $K^+ \subset$ *222*, X^- cryptates ($X^- = Cl^-$; Pic^-; PFO^-; CCD^-).

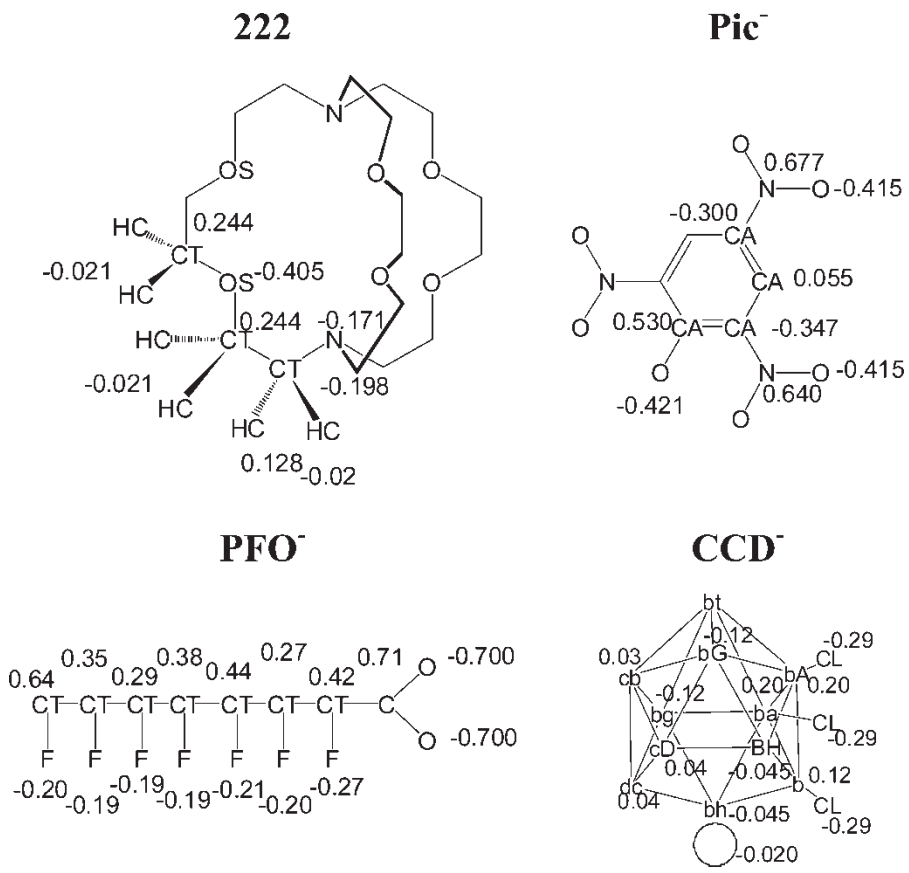

FIGURE 2 AMBER atom types and atomic charges used to simulate *222* and Pic^-, PFO^-, CCD^- ions.

(electrostatic + van der Waals) interactions between non-bonded atoms.

$$U = \Sigma_{bonds}K_r(r - r_{eq})^2 + \Sigma_{angles}K_\theta(\theta - \theta_{eq})^2 + \Sigma_{dihedrals}\Sigma_n V_n(1 + \cos n\phi) + \Sigma_{i<j}[q_iq_j/R_{ij} - 2\varepsilon_{ij}(R_{ij}^*/R_{ij})^6 + \varepsilon_{ij}(R_{ij}^*/R_{ij})^{12}]$$

The atom types and charges used for *222* and Pic^- (from refs. [34] and [35], respectively), PFO^- (charges derived from ESP potentials calculated with the 6-31G* basis set) are given in Fig. 2. The parameters of Na^+, K^+ and Cs^+ cations ($R^*_{Na} = 1.82$, $R^*_K = 2.65$, $R^*_{Cs} = 3.40$ Å; $\varepsilon_{Na=0.17}$, $\varepsilon_K = 0.00033$, $\varepsilon_{Cs} = 0.000081$ kcal/mol) were derived from the work ofÅqvist [36]. The CCD^- charges come from ref. [37], and the internal angle parameters of CCD^- have been adjusted to reduce the internal strain of the anion, and thus to better account for its diffusion at a given temperature. Water was represented with the TIP3P model [38]. For SC–CO_2, we used the three points model of Murthy *et al.*[39]: charges $q_C = 0.596$, $q_O = -0.298$ e and van der Waals parameters $R^*_O = 1.692$, $R^*_C = 1.563$Å and $\varepsilon_O = 0.165$, $\varepsilon_C = 0.058$ kcal/mol. All O–H, C–H bonds and the C═O bonds of CO_2 were constrained with SHAKE, using a time step of 2 fs. The intramolecular electrostatic and van der Waals 1–4 interactions were scaled down by a factor 2.0. Non-bonded interactions were calculated with an atom-based cutoff of 12 Å for all systems, using the PME-Ewald summation [40] to account for long range electrostatics. The non-bonded pair lists were updated every 25 steps.

The CO_2/water interface has been built as indicated in refs. [41,42] starting with adjacent "cubic" boxes of CO_2 and pure water of ≈30 to 60 Å

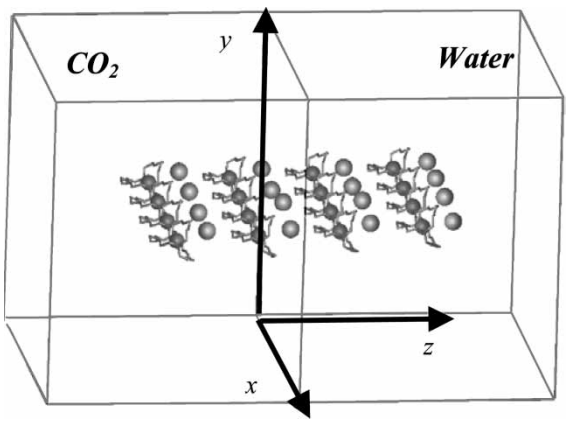

FIGURE 3 Simulation box with a grid of solutes initially "perpendicular" to the interface (system **H**).

TABLE I Characteristics of the simulated systems **A**–**S**

	Solute	Box Size (Å^3)	CO_2 + H_2O	Time (ns)
A	32 K^+ Cl^-	50 × 50 × (50 + 50)	1480 + 4249	2.5
B	32 K^+ Pic^-	60 × 60 × (50 + 50)	1595 + 4641	2.5
C	32 K^+ PFO^-	50 × 50 × (50 + 50)	1900 + 5778	2.5
D	32 K^+ CCD^-	55 × 55 × (47 + 47)	1608 + 4341	2.0
E	32 Cs^+ CCD^-	55 × 55 × (47 + 47)	1608 + 4341	2.0
F	32 Na^+ CCD^-	55 × 55 × (47 + 47)	1608 + 4341	2.0
G	16 222*	46 × 46 × (37 + 37)	792 + 2432	1.5
H	16 K^+ ⊂ 222 Cl -	45 × 45 × (37 + 37)	772 + 2446	2.5
I	16 K^+ ⊂ 222 Pic^-	45 × 45 × (37 + 37)	820 + 2471	2.5
J	16 K^+ ⊂ 222 PFO^-	45 × 45 × (37 + 37)	718 + 2341	2.5
K	16 K^+ ⊂ 222 CCD^-	52 × 52 × (30 + 50)	1312 + 2368	2.5
L	16 K^+ ⊂ 222 CCD^-	52 × 52 × (30 + 50)	926* + 2368	2.0
M	16 K^+ ⊂ 222 CCD^- + 16 222 + 16 K^+ CCD^-	60 × 60 × (30 + 30)	1001 + 3039	2.0
N	16 K^+ ⊂ 222 CCD^- + 16 222 + 16 K^+ CCD^-	50 × 50 × (72 + 8)†	1805 + 709	6.0
O	16 K^+ ⊂ 222 CCD^-	50 × 50 × (76 + 4)‡	1886 + 495	6.0
P	4 K^+ ⊂ 222 CCD	50 × 50 × (30 + 50)	1354 + 2328	1.5
Q	16 K^+ ⊂ 222···PFO^-	60 × 60 × (50 + 50)	1800 + 5430	2.0
R	16 K^+ ⊂ 222 PFO^- + 32 222	60 × 60 × (50 + 50)	1788 + 5046	2.0
S	16 K^+ ⊂ 222 PFO^- + 16 NEt_4^+ PFO^-	60 × 60 × (50 + 50)	1762 + 5192	2.0

*The organic phase is $CHCl_3$ instead of CO_2. (T = 350 K).
†90/10 CO_2/Water ratio ‡95 /5 CO_2/Water ratio.

length each for 50:50 mixtures (Fig. 3 and Table I). All systems were represented with 3D periodic boundary conditions, thus starting with alternating slabs of water and CO_2 separated by an interface. Initially, the solutes were immersed at the interface, equally shared between the two liquids, as shown Fig. 3.

After energy minimization, molecular dynamics "MD" was run at 350 K and constant volume for 50 ps with the solute frozen (in order to relax the solvent molecules), followed by 50 ps of free MD and by the production stage (≈1.6 to 6 ns). The temperature was monitored by coupling the system to a thermal bath at the reference temperature with a relaxation time of 0.2 ps using the Berendsen algorithm [43].

The results have been analyzed as described in refs [41,44] from the trajectories saved every 0.5 ps. The interface *z*-position was dynamically defined by the intersection of the solvent density curves. The percentage of species "at the interface" was calculated during the last 0.5 ns from the average number of species which sit within 8 Å from the interface, i.e. a distance corresponding to about half of the average interfacial width. When necessary, the two interfaces were considered. The definition of "interface" and "bulk" domains is somewhat arbitrary, but allows for consistent comparisons between different systems. The energy component analysis was performed in terms of pair wise additive contributions of the solvents (water and CO_2) and different solutes, using a 17 Å cutoff with a reaction field correction of the electrostatics [45]. Average energies, densities and radial distribution functions were averaged over the last 0.2 ns.

RESULTS

From the beginning to the end of the dynamics, the aqueous and CO_2 phases formed two distinct phases, linked by a fluctuating "interfacial slab" which is instantaneously non-planar and rough, with local important water/CO_2 mixing. We first describe the interfacial distribution of free K^+X^- and M^+ CCD^- salts (M^+ = Na^+; K^+; Cs^+). This is followed by a comparison of the K^+ cryptates with different counterions X^-, and simulation results on more complex systems. Interesting differences are observed, as far as the distribution of the ions and cryptates and their relationship with counterions are concerned.

The K^+X^- and M^+ CCD^- Electrolytes at the Interface

The simulations of K^+X^- and M^+ CCD^- salts (systems **A**–**F**) all started with a grid of solvent separated ion pairs at the interface, but finally lead to different distributions, depending on the nature of X^- in the first series (**A**–**D**), and on M^+ in the second one (**D**–**F**). They are consistent with both theoretical and experimental results according to which soft

TABLE II M^+X^- salts at the SC–CO_2/water interface (systems **A**–**F**): population of cations and anions at the interface, in water and in CO_2

	Ion	Interf. (%)	Water (%)	CO_2 (%)
A	**K^+**	28	72	0
	Cl^-	50	50	0
B	**K^+**	40	60	0
	Pic^-	65	35	0
C	**K^+**	55	45	0
	PFO^-	66	21	3
D	**K^+**	56	43	1
	CCD^-	75	22	3
E	**Na^+**	38	62	0
	CCD^-	55	45	0
F	**Cs^+**	69	27	4
	CCD^-	84	10	6

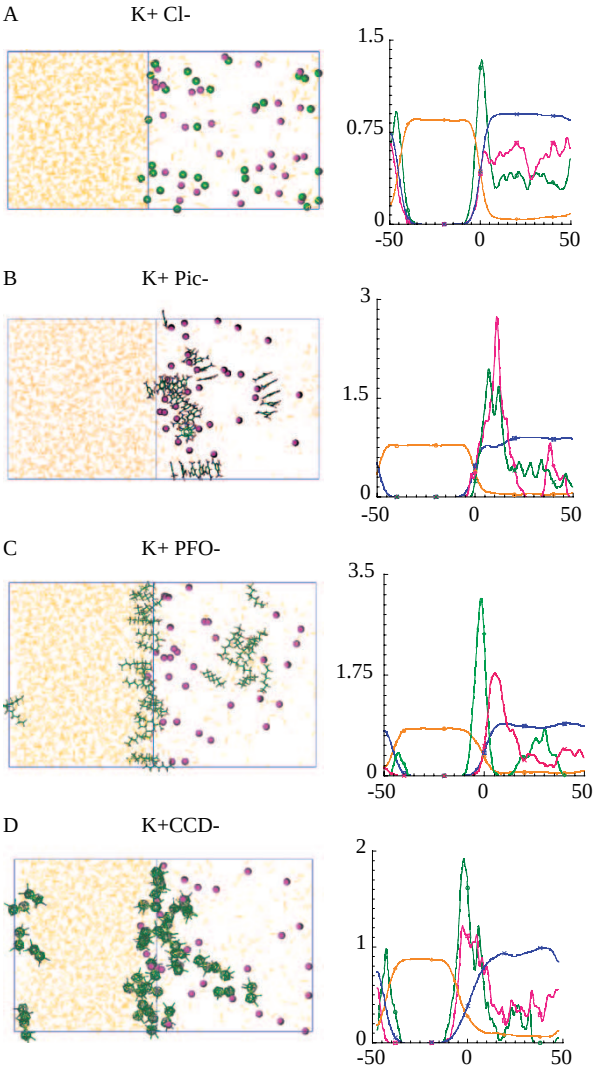

FIGURE 4 K^+X^- salts at the SC–CO_2/water interface (systems **A**–**F**). Final views (*left*, water not shown for clarity) and averages density curves (*right*. Colour coded with CO_2 in orange, water in blue, K^+ purple and CCD^- green).

polarizable anions reside at the surface of water, whereas hard cations prefer the aqueous phase [46–48]. The percentage of ions in the different phases is given in Table II.

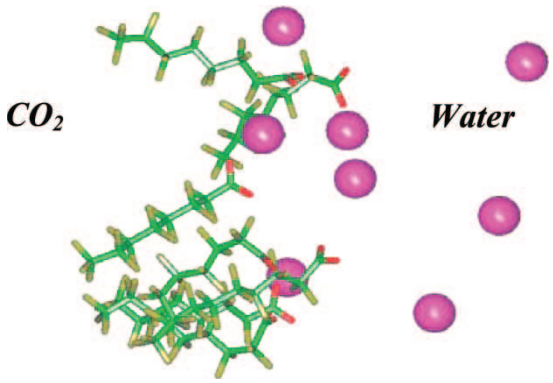

FIGURE 5 Zoom on PFO^- K^+ ions at the SC–CO_2/water interface (system **C**).

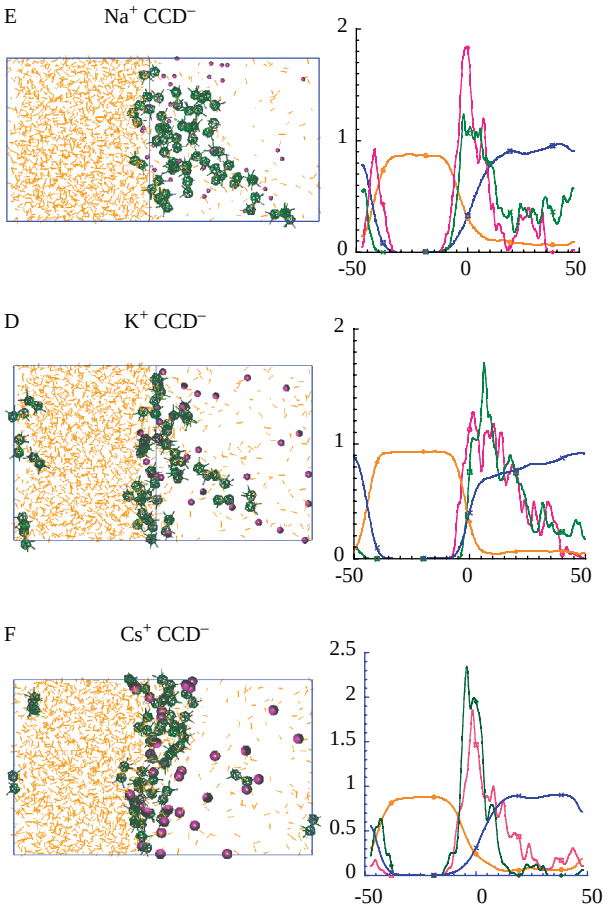

FIGURE 6 M^+ CCD^- salts at the SC–CO_2/water interface (systems **D**–**F**). *Left:* final view; *right*: average density profile along the z-axis. Colour coded with CO_2 in orange, water in blue, M^+ purple and CCD^- green.

Effect of Anions in the K^+X^- Series

Final distributions and density curves are shown in Fig. 4. As expected, the K^+ Cl^- salt is dissolved in the aqueous phase (72% of K^+ are in water) but Cl^- displays a quite high "affinity" for the interface (50% are adsorbed at the interface) which is consistent with theoretical results at the water/air interface [49]. At the end of the dynamics with the K^+ Pic^- salt, all Pic^- anions are also immersed on the water-side of the interface where they tend to self-assemble via π-stacking interactions, dynamically exchanging

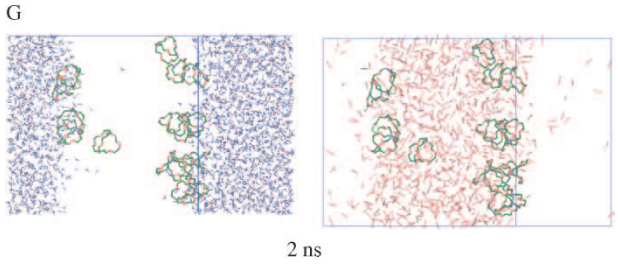

FIGURE 7 Free *222* cryptands at the SC–CO_2/water interface (system **G**). Final views, showing only water (left) and CO_2 (right) solvents for clarity.

TABLE III M^+X^- salts at the SC–CO_2/water interface (systems **A**–**F**): Average interaction energies and fluctuations (kcal/mol)

	X^-	E_{M^+/H_2O}	E_{X^-/H_2O}	E_{M^+/CO_2}	E_{X^-/CO_2}
A	K^+ Cl^-	−55.3 ± 2.9	−62.1 ± 6.6	−0.3 ± 0.0	−0.2 ± 0.1
B	K^+ Pic^-	−78.5 ± 6.9	−116.5 ± 4.1	−3.0 ± 0.4	−10.1 ± 1.5
C	K^+ PFO^-	−115.9 ± 3.6	−106.7 ± 2.1	−1.3 ± 0.3	−7.2 ± 0.5
D	K^+ CCD^-	−103.8 ± 3.5	−45.9 ± 2.1	−2.8 ± 0.4	−7.3 ± 0.4
E	Na^+ CCD^-	−110.7 ± 3.4	−61.6 ± 1.8	−1.6 ± 0.1	−6.3 ± 0.4
F	Cs^+ CCD^-	−76.1 ± 3.6	−39.3 ± 2.2	−3.6 ± 0.3	−8.2 ± 0.7

between stacks of 3 to 7 units. Some of them are in contact with the interface, leading to a broad peak of concentration (65%). The majority of K^+ cations are immersed in water, but again some of them (40%) sit at the interface, attracted by the interfacial Pic^- anions [50].

A similar behavior is observed with the K^+ PFO^- salts. Most of the PFO^- anions (66%) form a diluted interfacial layer, generally pointing their perfluoro chain to the CO_2 side and the carboxylate head to the water-side (Fig. 4). As a result, ≈ 55% of the K^+ cations concentrate at the interface, forming loose contact ion pairs with the carboxylates. A snapshot is given in Fig. 5. An energy component analysis (see Table III) reveals that the PFO^- anions are highly attracted by water (−107 kcal/mol), but somewhat less than are the Pic^- anions (−116 kcal/mol per anion). The per anion interaction energies with the CO_2 phase are much weaker (−7 kcal/mol for PFO^- and −10 kcal/mol for Pic^-). Perfluorinated chains are generally believed to be "sticky" and *all-trans*, therefore enhancing chain-chain interactions, but this is not the case here. A visual inspection shows many *gauche* dihedrals of PFO^- anions, presumably because the chains are not long enough and dense enough to pack, and because of shocks with solvent molecules.

Among the studied anions, CCD^- is expected to be most hydrophobic and, indeed, only 22% sit in water. The remaining ones concentrate at the interface, as found with classical organic solvents [51]. This is an interesting feature, given the non-amphiphilic structure of these anions. Like Pic^- anions, there are expelled out of water, in order to avoid paying for the high cavitation energy in water. On the other hand, they do not diffuse to CO_2 because at the interface they are strongly attracted by water (by −46 kcal/mol, on the average per CCD^- in system **D**; in pure water the attraction would be −87 kcal/mol) and by the K^+ cations which sit on the aqueous side of the interface. The fraction of cations "at the interface" (55%) is the same as with the amphiphilic PFO^- counterions.

Effect of Cations in the M^+ CCD^- Series

The cation effect on the distribution of M^+ CCD^- salts was studied with $M^+ = Na^+$, K^+ and Cs^+ (systems **D**–**F**) in relation with the Cs^+ extraction by CCD^- to classical organic solvents [30,52]. Final views and density curves are shown in Fig. 6. In the three studied systems, the anions form a film at the interface and the alkali cations sit in water. There are however subtle changes in their distribution, following a trend observed with the salts of hydrophobic anions S^- at the chloroform/water interface [53]. The cation concentration near the interface increases in the series Na^+(38%) < K^+(56%) < Cs^+(69%), i.e. with their decreasing hydration energies. The CCD^- anion concentration at the interface also increases in this series (55%, 75%, and 84%, respectively). The CCD^- anions generally interact with hydrated M^+ cations, without forming intimate CCD^- M^+ ion pairs.

We calculated the average area covered per CCD^- at the interface in the most "saturated interface", i.e. with the Cs^+ CCD^- salt (system **E**). The result (113 Å^2) is close to the value of 95 ± 8 Å^2 estimated experimentally at 293 K for the somewhat smaller dicarbollylcobaltate(III) anion (without chlorine substituents) at the water/dichloroethane interface in the presence of different mono- and di-charged metallic cations [54]. It was suggested that the symmetry axis of the anions is "parallel" to the interface, thus maximizing their interfacial area [54]. According to our simulations, a different picture emerges as the CCD^- anions adopt multiple orientations, without forming a saturated monolayer.

The 222 Cryptand and the $K^+ \subset$ *222*, X^- Cryptates with X^- = Cl^-/Pic^-/PFO^-/CCD^- Counterions

In this section, we describe the interfacial behavior of "concentrated solutions" containing 16 free *222* cryptands or 16 $K^+ \subset$ *222* complexes with different X^- counterions. Final snapshots are shown in Figs. 7–9. The distribution of cryptates and anions in the different phases is given in Table IV. Table V contains their average interaction energies with the two liquids.

The Uncomplexed 222 Cryptands Alone (system G)

As concerns the *222* cryptands, the majority (80%) adsorb at the CO_2 side of the interface(s) (see Fig. 7), thus displaying strong analogies with the chloroform/water

interface [55,56]. The other cryptands sit in CO_2 and dynamically exchange between the bulk and interfacial regions. Most cryptands retain their initial D_{3d}-type conformation, i.e. the same as in the K^+ complex. At the interface, they are hydrogen bonded to bridging water molecules, as found in bulk water [34] and at the chloroform interface [56]. As H-bonds are more labile at 350 K than at 300 K, one cryptand coordinates less water at the CO_2 interface than at the chloroform interface (1.3 versus 3.0 H_2O molecules on the average, respectively).

The $K^+ \subset$ 222, X^- Cryptates Alone

Depending on the counterion (systems **H**–**K**), different situations are observed, as far as the stability of the complexes and their distributions near the interface are concerned (see Fig. 8). With the Pic^-, PFO^-, CCD^- counterions, most of the cryptates remain stable during the dynamics, i.e. K^+ fluctuates near the center of the cavity of *222*. This contrasts with the Cl^- case, where three K^+ cations decomplexed, leaving two free cryptands in CO_2. Thus, *a first important effect of lipophilic anions is to enhance the stability of the complexes near the interface*, due to local electrostatic "neutralization" of the solution. Hydrophilic anions like Cl^- move to "bulk water", and the repulsions between the $K^+ \subset$ *222* species are therefore not compensated by attractions with X^-, thus destabilizing the complexes.[†]

In the systems **I** and **J** with Pic^- and PFO^- counterions, most anions and cryptates adsorb at the interface which is thus quasi-neutral. Only one Pic^- ion and one cryptate make short excursions to water. With PFO^- counterions, the interfacial landscape is similar, as 94% of the anions concentrate at an interface, contacting the aqueous phase via their carboxylate head. One observes an interesting difference between the Pic^- and PFO^- containing systems. In the former one, all solutes sit at a single interface, which was initially (at 0 ns) the nearest one. This contrasts with the more CO_2-philic PFO^- anions, which were able to migrate with cryptates through the CO_2 phase onto the other interface. With neither Pic^- nor PFO^- counterions do cryptates finally sit in CO_2. There is thus no K^+ extraction by *222*.

The CCD^- containing system **K** markedly differs as, after 2.5 ns of dynamics, the majority of the cryptates and their counterions sit on the CO_2-side of the interface, without direct contact with the aqueous phase (Figs. 8 and 9). They can thus be considered, at the microscopic level, as extracted. In contrast to the other anions containing systems, only a few complexes adsorb at the interface [10].

Given the analogies between SC–CO_2 and classical organic solvents used for liquid-liquid extraction purposes, we also simulated the same solute (16 $K^+ \subset$ *222*, CCD^-complexes; system **L**) at the aqueous interface with chloroform in the same conditions, i.e. at 350 K [11]. The results (Fig. 10) show a different behavior compared to the SC–CO_2 interface, as now all cryptates and counterions adsorb at the interface(s). None finally sits in the chloroform phase and there is thus no extraction to this liquid.

Mixtures of $K^+ \subset$ 222, CCD^- Cryptates, Uncomplexed 222 Cryptands and K^+ CCD^- Ions

The systems presented above contain a single type of solute, but real extraction systems involve an equilibrium between free and complexed ions. This is why we decided to model a solution containing a mixture of 16 [$K^+ \subset$ *222* cryptates, *222* cryptands, K^+ CCD^- ions]. In the absence of experimental information on the complexation constants at the interface, we arbitrarily chose a one to one ratio of the different species and a cubic box (system **M**). A snapshot of initial and final distributions can be seen in Fig. 11. After 2 ns of dynamics, one clearly sees that all cryptates are extracted to the CO_2 phase. None sits in water, and very few (15%) sit at the interface. Their extraction is concomitant with the high solubilization of CCD^- anions and cryptands in the CO_2 phase. At end of the dynamics, only two CCD^- and one *222* molecule sit in water close to the interface, while the majority (75%) of uncomplexed K^+ cations sit in water. The other cations sit at the interface, attracted by CCD^- anions.

Increasing of the CO_2/Water Ratio: Evolution from Well-defined Interfaces to Irregular Water "Droplets"

In an extraction experiment, the two phases separate due to external forces (e.g. centrifugation or gravity), gradually leading to macroscopically separated phases. In this section, we thus investigate the effect of increased CO_2/water ratio on the distribution of cryptates, choosing the most hydrophobic CCD^- anions. Two solutions of 16 $K^+ \subset$ *222*, CCD^- cryptates, with CO_2/water relative volumes of $\approx$ 90/10 and 95/5, respectively, have this been prepared, starting with a narrow water slab adjacent to a CO_2 slab (systems **N** and **O**) in which the solutes were immersed. The final distributions are shown in Fig. 12. It can be seen that the water domain is quite elongated, likely because the "rectangular" shape of the box favors attractive interactions with the images of water translated in the x,y directions (axes are

[†]*We also simulated the 16 K^+/222, Cl^- system, constraining K^+ at the center of the cavity of cryptands to prevent decomplexation. Again, most of the cryptates adsorbed at the starting interface, somewhat enhancing the interfacial Cl^- concentration (from 44 to 48%).*

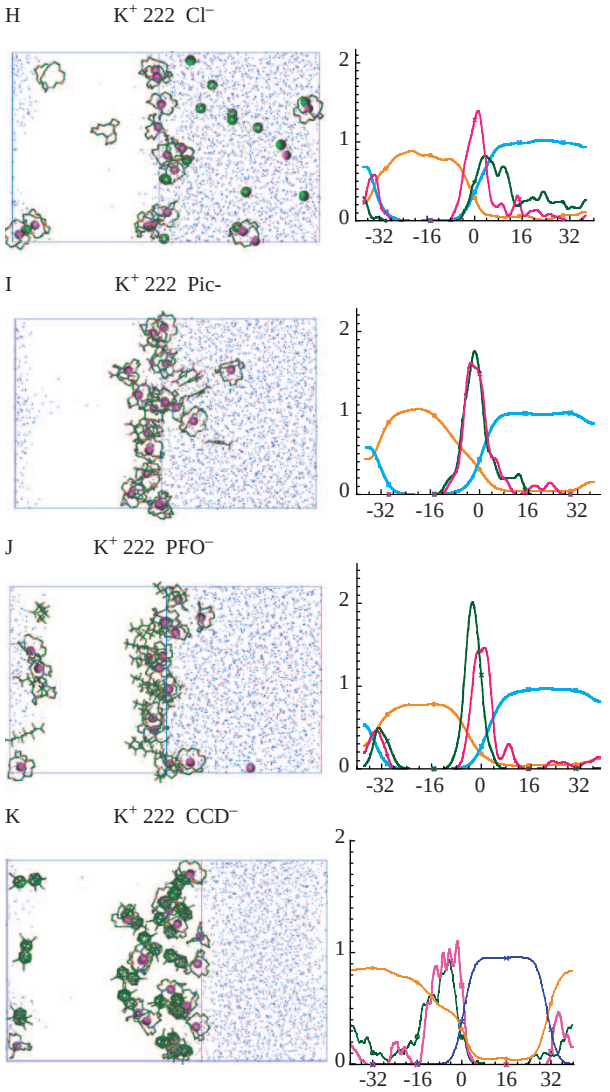

FIGURE 8 16 $K^+ \subset 222$ X^- cryptates at the SC–CO_2/water interface (systems **H–K**). Final views (*left*, CO_2 not shown for clarity) and average density curves (*right*). Colour coded with CO_2 in orange for, water in blue, K^+ purple and CCD^- green).

defined ion Fig. 3). This is why we decided to transform the box shape from "rectangular" to cubic during the dynamics, in order to make it more isotropic. This was achieved by 2 ns (system **N**) and

TABLE IV 16 $K^+ \subset 222$, X^- cryptates at the SC–CO_2/water interface (systems **H–K**): population of cryptates and anions at the interface, in water and in CO_2

	Ion	Interf. (%)	Water (%)	CO_2 (%)
H	$\mathbf{K^+ \subset 222}$	94	6	0
	$\mathbf{Cl^-}$	44	56	0
I	$\mathbf{K^+ \subset 222}$	88	6	6
	$\mathbf{Pic^-}$	88	6	6
J	$\mathbf{K^+ \subset 222}$	94	6	0
	$\mathbf{PFO^-}$	94	6	0
K	$\mathbf{K^+ \subset 222}$	63	37	0
	$\mathbf{CCD^-}$	63	37	0

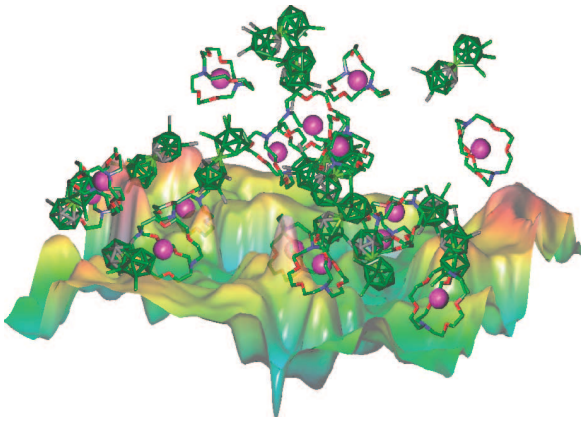

FIGURE 9 Snapshot of the surface of water (*bottom*) at the interface with CO_2 (*on top*), showing an equilibrium between adsorbed and "extracted" $K^+ \subset 222$ cryptates and CCD^- counterions (system **K**).

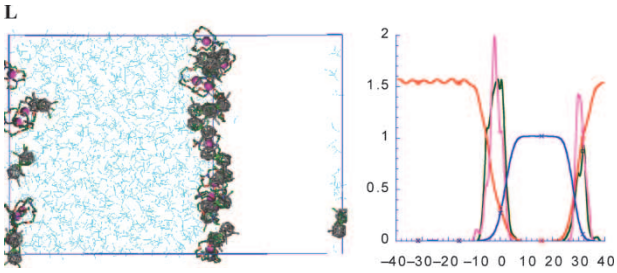

FIGURE 10 16 $K^+ \subset 222$ CCD^- cryptates at the water/chloroform interface (system **K**). Final views (*left*; water not shown for clarity) and average density profiles. Red: chloroform. Blue: water Green: CCD^-. Pink: K^+

6 ns (system **O**) of dynamics at constant volume, stepwise reducing the z-dimension and increasing the x,y dimensions of the box. It can be seen Fig. 12 that the final water domain is less elongated, without forming a regular "spherical" droplet, however. The average size of the droplet and distribution of solutes and CO_2 were estimated from the plot of radial distribution functions "RDFs" of water, K^+,

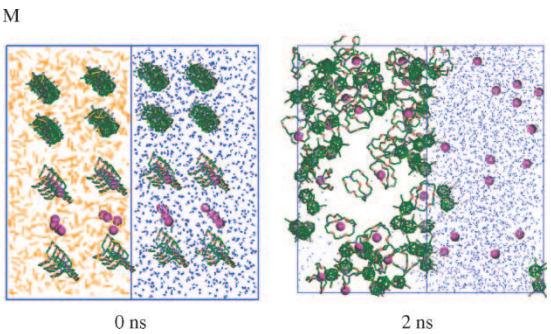

FIGURE 11 16 [222, $K^+ \subset 222$, CCD^-, K^+, CCD^-] species at the CO_2/water interface (system **M**): initial and final views.

TABLE V 16 $K^+ \subset 222$, X^- cryptates at the SC–CO_2/water interface (systems **H**–**K**): Average interaction energies and fluctuations (kcal/mol)

	X^-	$E_{222\subset K^+/H_2O}$	E_{X^-/H_2O}	$E_{222\subset K^+/CO_2}$	E_{X^-/CO_2}
H	**Cl^-**	-44.9 ± 1.3	-121.5 ± 4.3	-13.5 ± 0.8	-1.8 ± 0.3
I	**Pic^-**	-27.6 ± 1.8	-56.8 ± 4.3	-14.3 ± 0.9	-3.2 ± 0.8
J	**PFO^-**	-27.8 ± 1.2	-94.4 ± 3.8	-11.1 ± 0.6	-5.9 ± 0.7
K	**CCD^-**	-13.6 ± 1.5	-12.6 ± 0.9	-15.6 ± 0.5	-8.5 ± 0.5

Co(CCD) and CO_2 species around the dynamically defined center of mass of all water molecules (see Fig. 12). By analogy with the 50/50 mixtures, the "interface" between water and CO_2 was defined by the intersection of the water and CO_2 RDF curves, leading to average water droplets radii of $\approx$17Å for the 90/10 mixture and of $\approx$14Å for the 95/5 mixture. Thus, as expected, the size of the droplet decreases with the water content. As seen in Fig. 12, the water domain is instantaneously very irregular, and has different relationships with the solutes. Part of the water "surface" is in contact with "adsorbed" cryptates and CCD^- anions, while other parts are in contact with CO_2, as in the case of 50/50 mixtures. Integration of the RDFs indicates that within 8 Å apart from the "interface", one finds similar fractions of ions in the 90/10 and 95/5 mixtures: 63% and 60% of K^+ cryptates, respectively; 63% and 60% of CCD^- anions, respectively. Thus, the remaining cryptates (about 40%) are "extracted" to CO_2. This is similar to the fraction found above for the same system at the "planar interface" of the 50/50 mixture. Different cryptate—CCD^- relationships are observed in the CO_2 phase of the mixtures, where the ions may form loose contacts when K^+ is well "inclusive" and shielded from the solvent, or may be connected via water "fingers" involving K^+ hydration when K^+ is more facially complexed by *222* and solvated by one H_2O molecule.

DISCUSSION AND CONCLUSIONS

We report MD simulations on different extraction systems, performed consistently in terms of methodology, initial configurations and temperature. In all cases, the water and CO_2 phases are well identified and separated by an interfacial domain, but there are specific features, depending on the cation and complexant, which reveal the *importance of counterions*.

This is observed for the uncomplexed salts in the K^+X^- series ($X^- = Cl^-/Pic^-/PFO^-/CCD^-$), and in the M^+ CCD^- series containing hydrophilic alkali cations. The M^+ cation concentration on the aqueous side of the interface increases with the hydrophobicity and surface activity of X^-, and with the decreasing hydration energy of M^+. Upon complexation by the cryptand, the cation becomes hydrophobic, which is not sufficient, however, to induce its transfer to the CO_2 phase. In most cases, the cryptates adsorb and concentrate on the CO_2 side of the interface, because they are attracted by water and by the interfacial anionic layer.

The most remarkable result is the extraction of the $K^+ \subset 222$ complexes when CCD^- counterions are used. Extraction is computationally observed in a model system **K** containing only the complexes, as well as in a more realistic model **M** containing a mixture of cryptates, free ions and cryptands. At low concentrations, the complexes remain trapped at the interface (see Fig. 13 with system **P** containing only 4 $K^+ \subset 222$, CCD^- complexes) without diffusing to CO_2, and quasi-saturation of the interface is necessary to promote the extraction. Comparison of these systems demonstrates the *importance of ligand and anion concentration at the interface*. This can be considered as an "*interfacial synergistic effect*" of the CCD^- anions and of *222* ligands which are also surface active. Other hydrophobic and surface active species (e.g. concentrated CCD^- NR_4^+ salts, or co-solvents (e.g. fatty alcohols or tri-*n*-butyl phosphate "TBP") [57] may similarly act as synergists.

To our knowledge, there are no experimental data on cation extraction by cryptates to SC–CO_2, nor on the comparison of the studied anions. The results are however consistent with observed trends on related systems. Counterions are well known to influence the efficiency and selectivity in liquid-liquid extraction or transport to classical organic solvents [13,58–63]. Transport rate of salts by neutral macrocyclic carriers through hydrophobic membranes depends on the anion hydration energy, lipophilicity, and possible interactions with the crown ethers substituents [6,64]. The K^+ transport rates through chloroform follow the following order: $Pic^- > PF_6^- > ClO_4^- > IO_4^- > BF_4^- > I^- > SCN^- > NO_3^- > Br^- > BrO_3^- > Cl^- > OH^- > F^- > Acetate^- > SO_4^{2-}$, which is roughly the order of increasing hydration energies [64]. Note that a different counterion effect has been recently observed in ion extraction to room-temperature ionic liquids, which likely proceeds via an anion exchange with the ionic liquid, instead of anion co-extraction with the cation [65]. The aqueous $Lanthanide^{(III)}$ cation extraction to benzene by CMPO is greatly enhanced by adding small amounts of Pic^- anions [66]. The free energy of transfer from water to nitrobenzene increases in the series cobalt-

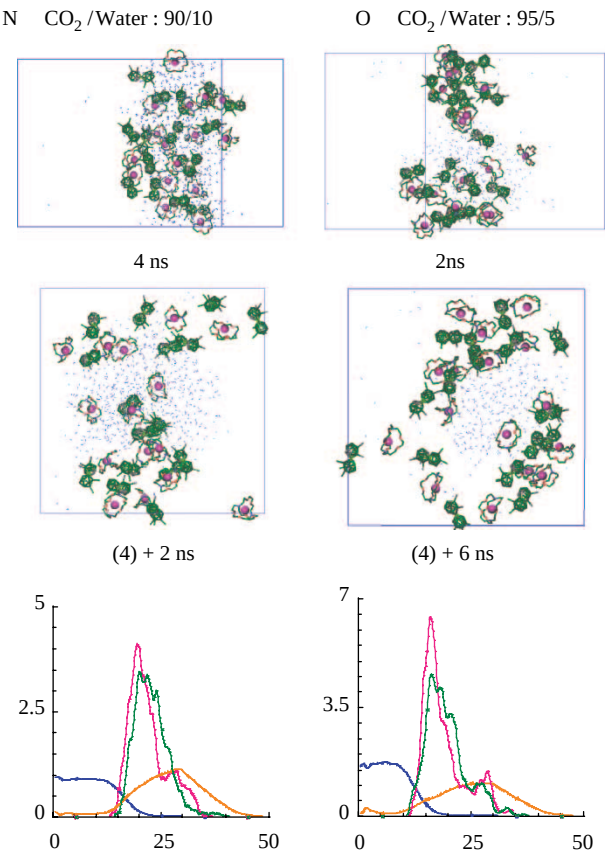

FIGURE 12 16 $K^+ \subset 222$, CCD^- cryptates in 90/10 (left) and 95/5 (right) water/CO_2 mixtures (systems **N** and **O**) simulated in a "rectangular" box (top) and in a "cubic" box (middle). CO_2 not shown for clarity. Bottom: radial distributions functions at water (blue), CO_2 (orange), K^+ cryptates (pink) and Co(CCD^-) (green) around the dynamically defined center of mass of water molecules.

dicarbollyl $<$ dipicrylaminate $<I_5^-$ $<BPh_4^-$ $<I_3^-$ $<$ Pic^- $<ClO_4^-$ $<I^-$ $<Br^-$ $<Cl^-$ [67,68], and we suggest that this is also the decreasing order of surface activity at aqueous interface. See also the role of counterions on the structure and properties of ionic micelles, whose charged surface displays clear analogies with liquid–liquid interfaces [69–73]. Our results are also consistent with vibrational sum frequency spectroscopy results, according to which

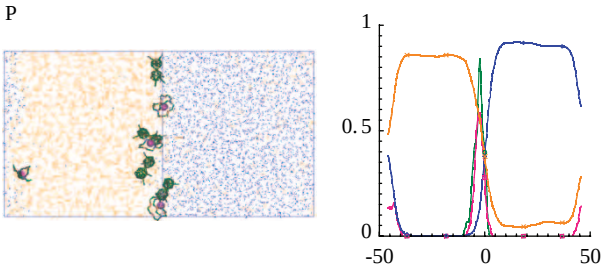

FIGURE 13 "Diluted solution" of 4 $K^+ \subset 222$ CCD^- cryptates at the water /chloroform interface (system **P**). Final views (*left*) and average density profiles (average over the last 200 ps). Red: Chloroform. Blue: water Green: CCD^- Pink: K^+.

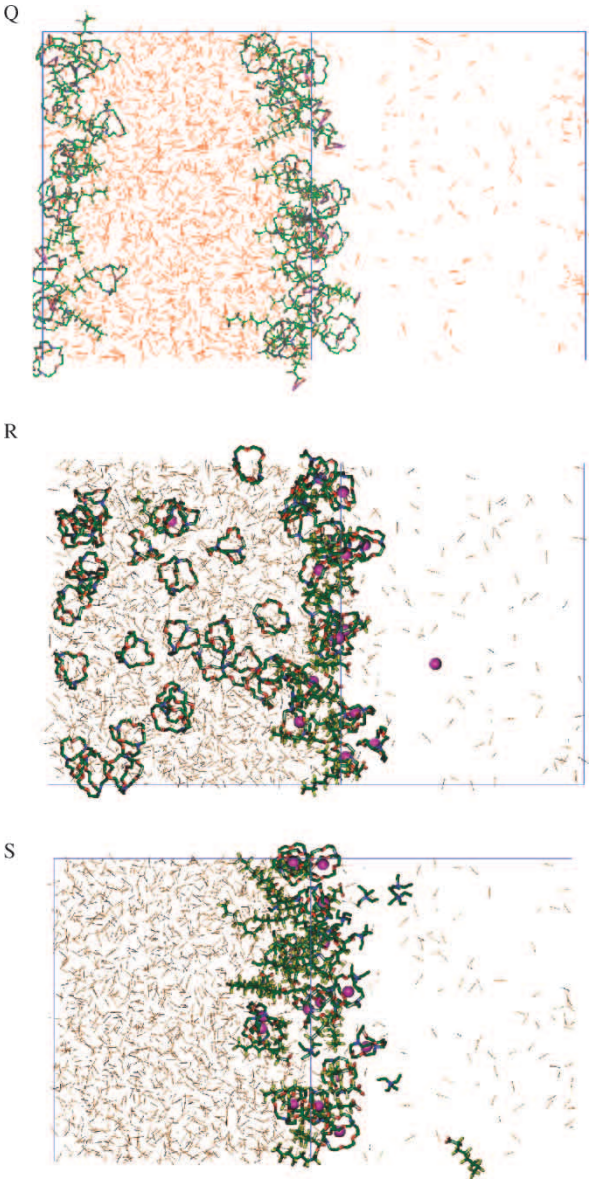

FIGURE 14 16 $K^+ \subset 222$ PFO^- cryptates at the CO_2/water interface (systems **Q**–**S**). From top to bottom: (i) simulations with "constrained" K-PFO bonds (**Q**), (ii) with an excess of 222 ligands (**R**), (iii) or of PFO^- $NEt4^+$ ions (**S**).

the surface activity of anions and their concentration in hydrophobic monolayers increase in the series SO_4^{2-} $>Cl^-$ $>NO_3^-$ $>Br^-$ $>I^-$ $>ClO_4^-$ $>SCN^-$ [74], also known as the Hofmeister series [75]. Concerning the K^+ extraction by 18C6 and its derivatives to SC–CO_2, the work of Mochizuki *et al.* [26] clearly demonstrates the enhancement resulting from the formation of 1:1:1 complexes of $K^+ \subset$ 18C6,PFO^- type, which is consistent with previous MD results [25]. Our study focuses on the aqueous interface, whose crossing is the key elementary step in classical, as well as in supercritical fluid extraction [76]. We note the similarity between the simulation results at classical and

supercritical interfaces. As seen here for the $K^+ \subset 222$,CCD^- complexes, there is however more adsorption at the chloroform than at the $SC-CO_2$ interface with water, presumably because of slower diffusion and lesser solvent mixing with chloroform. A discussion of counterion effects on ion distribution at classical aqueous interfaces can be found, e.g. in ref. [53]. Other issues, like the role of solvent polarity and polarizability deserve further investigations.

It is interesting to compare the effect of counterions on cation extraction to $SC-CO_2$ by 18C6 versus *222*. With the former ligand, K^+ and Sr^{2+} are efficiently extracted with PFO^- anions because the latter facially co-complex K^+ or Sr^{2+} via their carboxylate head, forming neutral complexes with intimate ion pairs. When complexed by *222*, the cation is more shielded than it is in the 18C6 complexes, and cannot form intimate ion pairs. As CCD^- anions are more hydrophobic and less surface active than are the PFO^- anions, their are more efficient for cryptates. Further proofs of the low efficiency of PFO^- anions to extract cryptates were obtained by three types of computer experiments based on the 16 $K^+ \subset 222$, PFO^- system. The results are shown in Fig. 14. The first system (**Q**) contains the 16 $K^+ \subset 222 \cdots PFO^-$ complexes in which counterions were constrained to form intimate ion pairs with K^+, in order to make the solutes still more hydrophobic. In fact, all constrained complexes adsorb at the interface(s). Some migrated through the CO_2 phase from one interface to the other, but none remained in "bulk" CO_2. There is thus no extraction with PFO^- counterions, in marked contrast to what is observed with CCD^- ones. The second variant solution (**R**) contains an excess of 16 *222* cryptands and the third one (**S**) an excess of 16 PFO^- Net_4^+ ions which may compete with the cryptates to saturate the interface, possibly promoting the extraction process. In fact, no extraction proceeds, as in the two systems **R** and **S** the cryptates remain trapped at the interface and are thus more surface active the free cryptands. When PFO^- Net_4^+ ions are added (**S**), one finds some cryptates on the CO_2-side of the interface, suggesting that a larger amount of CCD^- Net_4^+ salt might saturate the interface and promote the extraction.

To summarize, the simulations point to the importance of interfacial phenomena and of counterions in potassium extraction by cryptands to $SC-CO_2$, as in classical extraction. The CCD^- anions promote the $K^+ \subset 222$ extraction to CO_2 because (i) they are surface active and create a negative potential which attracts the cations near the interface. Otherwise, the cation would be "repelled" by the interface and could hardly be captured by the interfacial ligands [50]. (ii) The $K^+ \subset 222$ complexes are surface active and, at sufficiently high concentration, "saturate" the interface, which facilitates their migration to the CO_2 phase. As the water content diminishes, the systems evolve from "planar" interfaces to cylindrical or spherical water droplets of smaller surface area, which promotes the extraction to $SC-CO_2$. We hope that these investigations will stimulate experimental work on counterions effects at aqueous/supercritical fluid interfaces, as well as theoretical improvements concerning, e.g. the effect of system size and representation.

Acknowledgements

The authors are grateful to IDRIS, CINES and Université Louis Pasteur for computer resources and to PARIS for support. The authors thank E. Engler, A. Chaumont and G. Chevrot for assistance. NG thanks the French Ministry of Research for a grant.

References

[1] Dietrich, B.; Lehn, J. M.; Sauvage, J. P. *Tetrahedron Lett.* **1969**, *34*, 2889.
[2] Lehn, J. M. *Struct. Bonding* **1973**, *161*, 1–69.
[3] Kirch, M.; Lehn, J. M. *Angew. Chem. Int. Edit.* **1975**, *14*, 555–556.
[4] Kirch, M.; Lehn, J. -M. *Angew. Chem.* **1975**, 542–543.
[5] Lehn, J. M. *Acc. Chem. Res.* **1978**, *11*, 49–57.
[6] Lehn, J. M. In *Physical Chemistry of Transmembrane Ion Motions*; Spach, G., Ed.; Elsevier: Amsterdam, 1983; pp 181–206.
[7] Behr, J. P.; Kirch, M.; Lehn, J. -M. *J. Am. Chem. Soc.* **1985**, *107*, 241–246.
[8] Pedersen, C. J. *J. Am. Chem. Soc.* **1967**, *89*, 7017.
[9] Lehn, J. -M. *Angew. Chem., Int. Ed. Engl.* **1990**, *29*, 1304–1319.
[10] Lehn, J. -M. *Science* **1993**, *260*, 1762–1763.
[11] Cram, D. J. *Science* **1988**, *240*, 760–767.
[12] Koenig, K. E.; Lein, G. M.; Stuckler, P.; Kaneda, T.; Cram, D. J. *J. Am. Chem. Soc.* **1979**, *101*, 3553–3566.
[13] Moyer, B. A. In *Molecular Recognition: Receptors for Cationic Guests*; Atwood, J. L., Davies, J. E. D., McNicol, D. D., Vögtle, F., Lehn, J. -M., Eds.; Pergamon Elsevier: Oxford, 1996; pp 377–416.
[14] Izatt, R. M.; Clark, G. A.; Bradshaw, J. S.; Lamb, J. D.; Christensen, J. J. *Separation and Purification Methods* **1986**, *15*, 21–72.
[15] Lamb, J. D.; Izatt, R. M.; Christensen, J. J. In *Progress in Macrocylic Chemistry*; Izatt, R., Christensen, J. J., Eds.; Wiley: New York, 1981; p 42.
[16] Wai, C. M.; Wang, S. *J. Chromatogr. A* **1997**, *785*, 369–383.
[17] Lin, Y.; Smart, N. G.; Wai, C. M. *Environ. Sci. Technol.* **1995**, *29*, 2706–2708.
[18] Smart, N. G.; Carleson, T.; Kast, T.; Clifford, A. A.; Burford, M. D.; Wai, C. M. *Talanta* **1997**, *44*, 137–150.
[19] Carrott, M. J.; Waller, B. E.; Smart, N. G.; Wai, C. M. *Chem. Commun.* **1998**, 373–374.
[20] Erkey, C. *J. Supercrit. Fl.* **2000**, *17*, 259–287.
[21] Visser, A. E.; Swatloski, R. P.; Reichert, W. M.; Griffin, S. T.; Rogers, R. D. *Ind. Eng. Chem. Res.* **2000**, *39*, 3596–3604.
[22] Chun, S.; Dzyuba, S. V.; Bartsch, R. A. *Anal. Chem.* **2001**, *73*, 3737–3741.
[23] Wipff, G.; Kollman, P. A.; Lehn, J. -M. *J. Mol. Struct.* **1983**, *93*, 153.
[24] Lehn, J. M. *Angew. Chem. Int. Ed. Engl.* **1988**, *27*, 89–112.
[25] Vayssière, P.; Wipff, G. *Phys. Chem. Chem. Phys.* **2003**, *5*, 2842–2850.
[26] Mochizuki, S.; Wada, N.; Smith, R. L.; Inomata, H. *Analyst* **1999**, *124*, 1507–1511.
[27] Wai, C. M.; Kulyako, Y.; Yak, H. -K.; Chen, X.; Lee, S. -J. *Chem. Commun.* **1999**, 2533–2534.

[28] Cram, D. J.; Ho, S. P. *J. Am. Chem. Soc.* **1986**, *108*, 2998–3005.
[29] Plesek, J.; Grüner, B.; Hermanek, S.; Baca, J.; Marecek, V.; Janchenova, J.; Lhotsky, A.; Holub, K.; Selucky, P.; Rais, J.; Cisarova, I.; Caslavsky, J. *Polyhedron* **2002**, *21*, 975–986.
[30] Rais, J.; Selucky, P.; Kyrs, M. *J. Inorg. Nucl. Chem.* **1976**, *38*, 1376–1378.
[31] Rais, J.; Selucky, P. *Nucleon* **1992**, *1*, 17–20.
[32] Rais, J.; Grüner, B. In *Ion Exchange and Solvent Extraction*; Marcus, Y., SenGupta, A. K., Marinsky, J. A., Eds.; M. Dekker: New York, 2004; pp 243–334.
[33] Case, D. A.; Pearlman, D. A.; Caldwell, J. W.; Cheatham, III, T. E.; Wang, J.; Ross, W. S.; Simmerling, C. L.; Darden, T. A.; Merz, K. M.; Stanton, R. V.; Cheng, A. L.; Vincent, J. J.; Crowley, M.; Tsui, V.; Gohlke, H.; Radmer, P. J.; Pitera, J.; Massova, I.; Seibel, G. L.; Singh, U. C.; Weiner, P. K.; Kollman, P. A. *AMBER7*; University of California: San Francisco, 2002.
[34] Auffinger, P.; Wipff, G. *J. Am. Chem. Soc.* **1991**, *113*, 5976–5988.
[35] Troxler, L.; Harrowfield, J. M.; Wipff, G. *J. Phys. Chem. A* **1998**, *102*, 6821–6830.
[36] Åqvist, J. *J. Phys. Chem.* **1990**, *94*, 8021–8024.
[37] Stoyanov, E.; Smirnov, I.; Varnek, A.; Wipff, G. In *Euradwaste 1999: Radioactive Waste Management Strategies and Issues*; Davies, C., Ed.; European Commission: Brussels, 2000; pp 519–522.
[38] Jorgensen, W. L.; Chandrasekhar, J.; Madura, J. D.; Impey, R. W.; Klein, M. L. *J. Chem. Phys.* **1983**, *79*, 926–936.
[39] Singer, J. V. L.; Singer, K. *Mol. Phys.* **1972**, *24*, 357–390.
[40] Darden, T. A.; York, D. M.; Pede
rsen, L. G. *J. Chem. Phys.* **1993**, *98*, 10089.
[41] Wipff, G.; Engler, E.; Guilbaud, P.; Lauterbach, M.; Troxler, L.; Varnek, A. *New J. Chem.* **1996**, *20*, 403–417.
[42] Schurhammer, R.; Berny, F.; Wipff, G. *Phys. Chem. Chem. Phys.* **2001**, *3*, 647–656.
[43] Berendsen, H. J. C.; Postma, J. P. M.; van Gunsteren, W. F.; DiNola, A. *J. Chem. Phys.* **1984**, *81*, 3684–3690.
[44] Lauterbach, M.; Engler, E.; Muzet, N.; Troxler, L.; Wipff, G. *J. Phys. Chem. B* **1998**, *102*, 225–256.
[45] Tironi, I. G.; Sperb, R.; Smith, P. E.; van Gunsteren, W. F. *J. Chem. Phys.* **1995**, *102*, 5451–5459.
[46] Petersen, P. B.; Saykally, R. J. *Chem. Phys. Lett.* **2004**, *397*, 51–55.
[47] Lehr, L.; Zanni, M. T.; Frischkorn, C.; Weinkauf, R.; Neumark, D. M. *Science* **1999**, *284*, 635.
[48] Robertson, W. H.; Johnson, M. A. *Annu. Rev. Phys. Chem.* **2003**, *54*, 173.
[49] Dang, L. X.; Chang, T. -M. *J. Phys. chem. B* **2002**, *106*, 235–238.
[50] Berny, F.; Schurhammer, R.; Wipff, G. *Inorg. Chim. Acta* **2000**, *300–302*, 384–394.
[51] Coupez, B.; Wipff, G.; *C, R. Acad. Sci. Chim.* **2004**, *7*, 1153–1164.
[52] Teixidor, F.; Casensky, B.; Dozol, J. -F.; Grüner, B.; Mongeot, H.; Selucky, P. *European Commission, Nuclear Science and Technology*; *EUR 19956 EN* 2002; pp 188–193.
[53] Schnell, B.; Schurhammer, R.; Wipff, G. *J. Phys. Chem. B* **2004**, *108*, 2285–2294.
[54] Popov, A.; Borisova, T. *J. Colloid Interf.* **2001**, *236*, 20–27.
[55] Varnek, A.; Troxler, L.; Wipff, G. *Chem. Eur. J.* **1997**, *3*, 552–560.
[56] Jost, P.; Galand, N.; Schurhammer, R.; Wipff, G. *Phys. Chem. Chem. Phys.* **2002**, *4*, 335–344.
[57] Galand, N.; Wipff, G. *J. Phys. Chem. B* **2005**, *109*, 277–287.
[58] Yakshin, V. V.; Abashkim, V. M.; Laskorin, B. N. *Dokl. Acad. Nauk SSSR* **1980**, *252*, 373, Chem. Abs. 1980, 93, 102126h.
[59] Olsher, U.; Hankins, M. G.; Kim, Y. D.; Bartsch, R. A. *J. Am. Chem. Soc.* **1993**, *115*, 3370–3371.
[60] Hankins, M. G.; Bartsch, R. A.; Olsher, U. *Solvent Extr. Ion Exc.* **1995**, *13*, 983.
[61] Hiraoka, M. *Crown Compounds: Their Characteristics and Applications*; Elsevier: Amsterdam, 1982.
[62] Lindoy, L. F. *The Chemistry of Macrocyclic Ligand Complexes*; Cambridge University Press: New York, PortChester, 1990.
[63] McDowell, W. J. *Sep. Sci. Technol.* **1988**, *23*, 1251–1268.
[64] Lamb, J. D.; Christensen, J. J.; Izatt, S. R.; Bedke, K.; Astin, M. S.; Izatt, R. M. *J. Am. Chem. Soc.* **1980**, *102*, 3399–3403.
[65] Dai, S.; Ju, Y. H.; Barnes, C. E. *J. Chem. Soc. Dalton Trans.* **1999**, 1201–1202.
[66] Naganawa, H.; Suzuki, H.; Tachimori, S.; Nasu, A.; Sekine, T. *Phys. Chem. Chem. Phys.* **2001**, 2509–2517.
[67] Girault, H. H.; Schiffrin, D. J. In *Electroanalytical Chemistry*; Bard, A. J., Ed.; Dekker: New York, 1989; pp 1–141.
[68] Koryta, J.; Vanysek, P.; Brezina, M. *J. Electroanal. Chem.* **1977**, *75*, 211–228.
[69] Aswal, V. K.; Goyal, P. S. *Chem. Phys. lett.* **2002**, *357*, 491–497.
[70] Askal, V. K.; Goyal, P. S. *Chem. Phys. Lett.* **2003**, *368*, 59–65.
[71] Srinivasan, V.; Blankschtein, D. *Langmuir* **2003**, *19*, 9932–9945.
[72] Srinivasan, V.; Blankschtein, D. *Langmuir* **2003**, *19*, 9946–9961.
[73] Bales, B. L.; Tiguida, K.; Zana, R. *J. Phys. Chem. B* **2004**, *108*, 14948–14955.
[74] Gurau, M. C.; Lim, S. M.; Castellana, E. T.; Albertorio, F.; Kataoka, S.; Cremer, P. S. *J. Am. Chem. Soc.* **2004**, *126*, 10522–10523.
[75] Hofmeister, F. *N.-S. Arch. Exp. Path. Pharmakol.* **1888**, *24*, 247–260.
[76] Watarai, H. *Trends Anal. Chem.* **1993**, *12*, 313–318.